Title
Observations concerning the quinol oxidation site of the cytochrome bc{sub 1} complex

Journal
Federation of European Biochemical Societies, 555(1)

Authors
Berry, Edward A.
Huang, Li-Shar

Publication Date
2003-09-07

Observations concerning the quinol oxidation site of the cytochrome bc_1 complex.

Edward A. Berry*[§] and Li-shar Huang[§]

[§]Lawrence Berkeley National Lab

Keywords: ubiquinone, cytochrome c, oxidoreductase, membrane protein complex, respiratory enzyme, protein crystal, x-ray, structure, mechanism, tautomerism, resonance.

*Corresponding author

Email: EABerry@LBL.gov

Fax: 1-510-588-4829

Address:

MS 64R121

Lawrence Berkeley National Laboratory

Berkeley, CA 94720

USA

[1]Abbreviations used: cyt., cytochrome; EPR, electron paramagnetic resonance; Q_O and Q_I, quinol oxidation and reduction sites proposed by protonmotive Q-cycle hypothesis; N and P, sides of energy transducing membrane that become negative and positive upon energization.

Abstract. A direct hydrogen bond between ubiquinone/quinol bound at the Q_O site and a cluster-ligand histidine of the iron-sulfur protein (ISP) is described as a major determining factor explaining much experimental data on position of the ISP ectodomain, EPR lineshape and midpoint potential of the iron-sulfur cluster, and the mechanism of the bifurcated electron transfer from ubiquinol to the high and low potential chains of the bc_1 complex.

Introduction. The cytochrome *bc1* complex (ubiquinol:cytochrome c oxidoreductase, E.C.1.10.2.2) is the middle section of the respiratory chain of mitochondria and many bacteria. It oxidizes ubiquinol and reduces a small soluble cytochrome c. Part of the free energy released is coupled to development of a transmembrane gradient in the electrochemical potential of the hydrogen ion, which serves as the energy source for a number of other processes including ATP synthesis. The mitochondrial complex is a homodimer of monomers consisting of 10 or 11 different subunits. At the time of the previous Nobel symposium on membrane proteins, a three-dimensional model at around 20 Å was available from electron microscopy/image reconstruction [1]. Over the past decade x-ray crystallographic structures of the *bc1* complex have become available at successively higher resolution and completeness [2-10] so we now have a fairly detailed understanding of the structure of the mitochondrial enzyme. In collaboration with Fevzi Daldal we are currently determining the structure of the cyt.[1] *bc1* complex from *Rhodobacter capsulatus*. The overall structures of the mitochondrial and bacterial enzymes are shown in Figure 1.

Although protein architecture is certainly interesting for its own sake, the major

impetus for the structural studies of the respiratory complexes has been to further our understanding of how these enzymes work. In contrast to the situation with cytochrome oxidase, a widely accepted mechanism to account for the detailed stoichiometry of charge and proton translocation by the bc_1 complex was available before the first crystal structure emerged. Therefore the role of the structural studies in elucidating the function has not been to provide hints of possible mechanisms but rather to confirm (or refute) predictions of this model (Mitchell's protonmotive Q-cycle mechanism [11,12]) and to elucidate in detail how the protein meets the postulates required by the mechanism.

The crystallographic structures have for the most part confirmed the predictions made by the Q-cycle mechanism, and have not turned up any details inconsistent with that mechanism. Disappointingly none of the structures has revealed quinone in any form at the Q_O site, and this is certainly a goal to strive for, however the failure so far can readily be explained by the facts that the best structures are from preparations with low quinone content and/or are obtained in the presence of tight-binding Q_O-site inhibitors that displace quinone. So for modeling the Q_O-site reaction we have to rely on models of quinoid inhibitors bound at the site and on comparisons with quinone binding sites in other structures. Quinone analogs whose binding at the Q_O sight has been described from high-resolution structures include stigmatellin, HHDBT [13], HQNO [10], and famoxadone [9]. For comparison structures of the *B. viridis* reaction center are available [14] with quinone (entry 2PRC) or stigmatellin (4PRC) at the Q_B site.

A new crystal form of the vertebrate cytochrome bc_1 complex. Our latest additions to this series of structures are obtained from a new crystal form of the bovine enzyme in the

orthorhombic space group $P2_12_12_1$ (cell edges about $130 \times 175 \times 230$) with a dimer in the asymmetric unit. The crystals diffract to beyond 2.0 Å, but at present the high mosaicity limits accurate data to around 2.1 A. We have recently deposited structures 1PP9 (with stigmatellin at the Q_O site) and 1PPJ (with stigmatellin and antimycin bound). A manuscript describing the details of these structures and comparing with previous structures is being prepared. Here we present only the binding of stigmatellin at the Q_O site (Figure 2) as a model for ubiquinone binding.

Binding mode of ubiquinone and quinoid inhibitors at the Q_O site. Shortly after evidence began to mount that the iron-sulfur cluster had nitrogenous as well as sulfur ligands [15,16], it was proposed by Rich [17] and Robertson et al. [18] that one of the ligands for quinone/quinol at the Q_O site was a histidine serving also as ligand for the Fe_2S_2 cluster. These proposals were based partly on analogy with the Q_A and Q_B sites of bacterial photosynthetic reaction centers, but also on the changes in EPR spectra and midpoint potential of the ISP depending on the occupant of Q_O, which will be discussed below and were seen as evidence of a close interaction between the cluster and the occupant of the Q_O site.

The presence of a strong hydrogen bond between the Q_O-site occupant and a histidine ligand of the ISP center was confirmed at least in the case of stigmatellin in 1998 when Zhang et al. [4] reported this hydrogen bond in the crystal structure of the stigmatellin-loaded avian *bc_1* complex. It has since been observed in the fungal [7] and bovine (this work) complexes with stigmatellin, in the fungal complex with another inhibitor HHDBT [13], and recently in a bovine complex with NQNO [10].

In this paper we argue that this strong H-bond between the ISP cluster-ligand

histidine and substrate or inhibitor bound in a pocket of cyt. *b* is central to the explanation of a body of inter-related phenomena concerning the effects of redox state, Q_O-site inhibitors, and site-directed mutations in the ISP "neck" region on the resting position, midpoint potential, and EPR lineshape of the ISP. And we propose that the redox properties of the complex between the ISP and quinone at the Q_O site could be sufficient to ensure the bifurcated electron transfer at the Q_O site.

Figure 2A shows the headgroup of stigmatellin and surrounding residues of the binding pocket from our structure 1PPJ. Previous structures of the chicken (2bcc) and fungal (1ezv, 1kb9) complexes have the same binding mode. The headgroup is suspended by strong H-bonds on either side of the ring. One connects the phenolic OH to Glu271 of cyt. *b*. The other connects the carbonyl oxygen to Nε2 of His161 in the ISP. The two stigmatellin methoxy oxygens are within H-bonding distance of the same residues (His161 and Glu272) but with relatively long bond lengths (3.4-3.5 Å vs 2.6-2.7 Å for the strong bonds mentioned above). The phenolic OH is further bonded through a water molecule to the other carboxylate oxygen of Glu271. Otherwise the binding appears to be Van der Waals and hydrophobic, involving in particular Leu121, Met129, Phe274, and Tyr278. The close contact of the related inhibitor HHDBT with Tyr279 (corresponding to tyr278 in the beef sequence) has been proposed [13] to represent a weak, edge-on aromatic H-bond , and the same argument could be made here.

The interaction with His161 is similar to the interaction between stigmatellin at the Q_B site and His L190 in the *B. viridis* reaction center (PDB entry 4PRC) except that in that case the histidine Nδ1 atom binds stigmatellin and Nε2 binds the iron atom, while in the bc_1 structure the histidine ring N's have their roles reversed. H-bond distances from

the ring N to stigmatellin carbonyl and methoxy oxygens are 2.72 and 3.06 Å in 4PRC, versus 2.64 and 3.48 Å in 1PPJ.

It is generally assumed that quinone in at least some of its redox states and some part of the catalytic cycle, binds in the manner of stigmatellin, H-bonded between His161 of the ISP and E271 of cyt. *b*. Figure 2B shows ubiquinone modeled into the density of stigmatellin, on the assumption that stigmatellin binds as a ubiquinone analog and hence must present a similar shape to the binding pocket. The fit is quite good for the headgroup, with the five of the six ring substituents fitting into lobes of density from the corresponding substituents of stigmatellin. The isoprenoid tail does not fit well, however there is a lot of room here and the tail in the ubiquinone model makes no clashes.

The relative orientation of ubiquinone and stigmatellin depicted here is the same as in the Q_B site of the reaction center based on entries 4PRC and 2PRC, that is with the carbonyl O4 atom of ubiquinone (2,3 dimethoxy 5 methyl 6-polyisoprenyl 1,4-benzoquinone) and the carbonyl O4 of stigmatellin oriented toward the His ligand.

EPR Lineshape of the ISP Fe_2S_2 cluster: Primarily an indicator for the presence or absence of an H-bond between cluster-ligand His161 of the ISP and the occupant of the Q_O site? A number of early EPR studies summarized [19] indicated an interaction of the ISP Fe_2S_2 cluster with oxidized quinone or Q_O-site inhibitors resulting in altered ISP lineshape. In later years these results were extended to different inhibitors [20], quinone-depleted membranes [21], isolated soluble form of the ISP [22], and mutated complexes [23]. The EPR spectrum of the isolated extrinsic, functional domain (ectodomain) of the ISP shows a broad g_x band at g=1.76. A similar spectrum is obtained in the entire

complex at low potentials where quinone is reduced or when quinone is absent due to extraction, genetic manipulation, or the presence of inhibitors such as myxothiazol which displace quinone and do not themselves interact with the ISP.

In the presence of oxidized quinone all the g-values are shifted, the g_x being most characteristic. The g_x band sharpens and shifts to 1.80 when there is quinone in the Q_O site. Several Q_O-site inhibitors have similar effects. Stigmatellin for example results in a greatly sharpened g_x peak shifted to 1.79. It seems safe to see the sharpened g_x band at ~1.79 as an indication that the ISP ectodomain is H-bonded to the occupant of the Q_O site. From what we know of the structure of the Q_O site this implies that the ectodomain is in the B position (see below). The precise g-value and bandwidth is an indication of what that occupant is. More refined analysis may tell something about the environment of the Q_O site, such as the presence of a second quinone [21], but the most obvious and major factor affecting the lineshape is the presence or absence of this H-bond between the ISP and the Q_O site occupant.

Movement of the ectodomain of the iron-sulfur protein in the catalytic cycle. One finding that came out of the structures, and that was neither required nor expected from the Q-cycle model, was the fact that the ectodomain of the ISP was found in at least two different positions, one with the Fe_2S_2 cluster near the presumed Q_O quinone binding site and one near cyt. c_1 [4]. Since neither of the positions was close enough to both of these redox partners to allow electron transfer at the observed rates from a single site, it was inferred that electron transfer between these centers depended upon mobility of the ISP as part of the reaction cycle. The position in proximity to the Q_O sites is referred to as the

proximal or "B" position, and the position close to cyt. c_1 as the distal or "C" position.

This raised a number of questions not directly related to the Q-cycle mechanism, but rather to the motion of the ISP. Is the motion between the two sites driven by the conformational changes in the rest of the complex, or is it passive diffusion between the sites (Figure 3)? If it is driven, do conformational changes exert force directly on the ectodomain to move it between positions, or do conformational changes adjust the affinity of one or both binding sites so that by passive diffusion most of the ISP ends up in one condition? What experimental factors affect the position of the ectodomain in the resting enzyme? What techniques can we use to ascertain the resting position if not in a crystalline state?

In the crystals the ectodomain position is affected by the presence and species of Q_O-site inhibitors [4,5]. This was explained based on random diffusion between binding sites of different affinity, with the affinity of the B position determined largely by the availability and strength of the H-bond between the Q_O-site occupant and His161 [24]. This still seems to be the best explanation of most of the crystal data on movement.

Orientation-dependent EPR spectroscopy of oriented films of protein was used to demonstrate changes in position as a function of redox state of the Fe_2S_2 center and another component presumed to be quinone at the Q_O site [25]. In order to apply this technique to the oxidized cluster, which is not paramagnetic, the sample was reduced by γ-irradiation after fixing the position by drying and freezing. We interpret the redox dependence by supposing that a strong H-bond is formed between the reduced ISP and oxidized quinone, but not between the two species when both are reduced or both are oxidized. This is supported by the effect of redox state on the EPR lineshape of the

cluster, discussed above.

Redox midpoint potential of the ISP cluster. The midpoint potential of the ISP is affected by Q_O-site inhibitors. Most dramatically, stigmatellin raises it by ~250 mv [20]. This was attributed to stigmatellin binding to the reduced ISP some 17,000 times more tightly than to the oxidized. Other inhibitors raise the midpoint potential by lesser amounts [26], while DBMIB lowers it [27], implying tighter binding to the oxidized form.

All of this was understood before the structures were determined or movement of the ectodomain was suspected. A recent paper from Crofts and coworkers [28] extends the model to include equilibria between different positions of the ectodomain and competition with endogenous quinone. MOA inhibitors [29] such as myxothiazol lower the midpoint slightly but leave the line shape similar to that of the isolated ectodomain. It seems likely that their effect is due to displacement of quinone, which apparently, like stigmatellin, binds to the reduced ISP more tightly albeit by a smaller margin.

Since the inhibitor can only bind to ISP in the B position, anything that affects the equilibrium between the B and C positions may also affect the midpoint potential. This may explain the effect of genetically engineered insertions and deletions in the "neck region" of the ISP on activity and midpoint potential of the ISP cluster. Insertion of a few residues results in an inactive complex. From the EPR lineshape, the ISP resides mainly in the B position bound to quinone. As discussed in reference [30], one explanation involves the fact that rotation of the ectodomain to the B position results in stretching the neck region and partially uncoiling a helix in this region. It may be that this helix serves

as a "spring" to keep some tension pulling the ectodomain out of the B position, promoting dissociation of the product complex. Lengthening the neck region weakens the tension and the complex dwells with the ISP in position B too long to be kinetically competent.

Enforced bifurcation of electron transfer to the high and low potential chains upon oxidation of quinol at the Q_O site. This so-called "bifurcated reaction" is required by the Q-cycle mechanism to account for the observed proton and charge translocation stoichiometry, which results in conservation of a large part of the free energy available in the reaction. One electron passes via the iron-sulfur protein and cyt. c_1 to cyt. c (the "high potential chain"), providing the driving force for the reaction. The other electron is recycled via the *b* cytochromes to reduce quinone back to quinol.

This halves the number of low potential electrons consumed per turnover, and due to the fact that quinone reduction site is in protonic equilibrium with the N side of the membrane, provides the proton uptake mechanism of the proton pump. If both electrons took the thermodynamically favorable path down the high potential chain, the bc_1 complex would be half a Mitchellian protonmotive loop and could pump no protons by itself. And if the electrons were free to go independently and reversibly by both pathways, it would enable futile cycles that would drain off the proton gradient produced by the other complexes.

To the extent that we accept the model for quinone binding presented in Figure 2B, the x-ray structures set the stage in which the bifurcated reaction must take place. Although the binding pocket for quinone is in cyt. *b*, one of its strongest ligands is

His161 of the iron-sulfur protein. His161 directly ligates the Fe_2S_2 cluster of the iron-sulfur protein, and thus is a part of the π-orbital system through which the unpaired electron of the reduced ISP is delocalized (Figure 4).

Thus the π-orbital systems of the two reacting centers ubiquinone and the Fe_2S_2 cluster are separated by a single strong hydrogen bond, with atom-to-atom distance of 2.8 Å in the model of Figure 2. While the non-adiabatic tunneling mechanism is not applicable at such short distances, application of the "Dutton Ruler", equation 3 of [31], with $\Delta G = -\lambda$ to get an order-of-magnitude estimate leads to predicted electron transfer rates of greater than $10^{13}s^{-1}$, i.e. fast on the EPR time scale ($10^{9}s^{-1}$) and extremely fast compared to the maximal observed rate for the Q_O site reaction [32]. Thus on the time scale we are interested in, it might be more realistic to consider the electron is delocalized over both centers.

The actual mechanism might involve a bond-rearrangement tautomerism as suggested by Rich [33] for the transfer of H° through histidine. A possible scheme of bond rearrangements is indicated in Figure 4. If the complex is a resonance hybrid of two or more tautomers, this would allow partial transfer of the electron between the two centers depending on the relative stability of the tautomers.

Note that it is assumed that quinol is the H-bond donor and His161 the acceptor, in contrast to previous models [18,33,34]. This does not imply the need for deprotonation of either quinol or the ISP before binding, rather the initial complex may have quinol accepting followed by dissociation of the proton not involved in the H-bond. In any case the result is a strong, short H-bond between groups both having pKa's above neutrality. The transition state may involve a symmetrical H-bond of the type described [35,36].

Robertson et al. [18] suggested that the strong orbital overlap between quinone, ISP cluster, and cyt. *b* in their model of quinone binding would be important for the kind of concerted mechanism proposed by Meinhardt and Crofts [37] for the quinol oxidation reaction. The present paper can be seen as an extension of that idea in light of the evidence that the ISP is, but heme *b* is not, involved in ligating quinone.

The reaction complex, or enzyme-substrate complex, is formed by binding of oxidized ISP to ubiquinol at the Q_O site. Note that this is different from (having one less electron than) the complex between reduced ISP and quinol which we supposed not to form in order to explain the ISP position and lineshape at low redox potential. Unfortunately little is known about it. It is presumably transient except under conditions where cyt. *b* is fully reduced and the high potential chain oxidized (as in the "oxidant induced reduction" experiments). Neither the reduced quinol nor the oxidized Fe_2S_2 cluster are paramagnetic, and even if one electron resides on the ISP in the reaction complex, spin coupling between the semiquinone and ISP electrons would abolish the EPR spectrum.

On the other hand a good deal is known about the product complex between oxidized quinone and the reduced ISP, which is paramagnetic and has been studied extensively by EPR spectroscopy. As summarized above, a large body of data on the effects of inhibitors and redox state on the lineshape and redox midpoint potential of the ISP can be explained at least qualitatively based on the existence or not of an H-bond between the Q_O-site occupant and the reduced ISP. We would thus say that the sharpened g_x=1.80 lineshape is the signature of the product complex. Furthermore it seems reasonable to view the crystal structure with stigmatellin's carbonyl oxygen H-bonded to

the reduced ISP as an analog of the product complex.

The enzyme-substrate or reaction complex, formed by reduced quinone and oxidized ISP, is formally a reduced form of this product complex. To emphasize this fact we can call the H-bonded complex of the ISP with quinone or quinol the "R-complex". I will refer to the product complex as the oxidized or one-electron form of the R-complex, and the reaction complex as the reduced or two-electron R-complex. The fully reduced, three-electron complex between reduced ISP and quinol does not form, which is the reason for the disappearance of the g_x=1.8 signal and the movement of the ISP ectodomain at low redox potential.

One way of describing the proposed mechanism is to say that the first electron from quinol is transferred to cyt. *b*, not the ISP (but see below). The distance from the Q_O site to heme b_L is 10 Å edge to edge, consistent with the turnover rate and measured rate constants provided the ΔG is not too unfavorable and the reductant species is present at high occupancy. Such models have been rejected in the past because of the extreme instability of the semiquinone species at the Q_O site, which would make ubiquinol a poor 1-electron reductant and the ΔG for the reaction highly unfavorable. We propose that even though quinol may be a poor one-electron reductant, the reduced R-complex (consisting of quinol complexed to the oxidized ISP) is a good one electron reductant, because the product is not unstable semiquinone but rather the oxidized R-complex, a stable complex that can be observed by EPR to form at high occupancy from reduced ISP and oxidized ubiquinone or quinone analog inhibitors.

However it is not quite right to say that the first electron goes to cyt. *b*, because the electron is transferred to cyt. *b* from the reduced R-complex, and we don't know where

the electrons are in that. We suggested above that electrons could be delocalized on the reaction time scale between the Fe_2S_2 center and the quinoid system via the H-bond. If in fact one electron from the substrate quinol resides mainly on the Fe_2S_2 center in the reduced R-complex, then we have the spin-coupled complex of semiquinone and reduced ISP described by Link [34]. If there is very little electron transfer from quinol to ISP in the reduced R-complex, but the cloud of the second electron sloshes over to the Fe_2S_2 center concomitantly with the transfer of the first electron to cyt. *b*, then we have a concerted mechanism as proposed by Meinhardt and Crofts [37] and by Snyder et al. [38].

Once the oxidized R-complex is formed and relaxes to its ground state, it is pretty clear from the EPR spectrum that the unpaired electron is on the ISP cluster. However it is tempting to speculate that the sharpening and shifting to higher g-values is indicative of mixing in some radical g=2.0 signal due to a minor occupancy on the semiquinone. Slightly different spectral effects of quinone and different inhibitors on the ISP spectrum would be due to the different environment of the electron on the different quinoid systems, as well as different distribution between quinone and Fe_2S_2 cluster.

It is a truism that the reaction complex is the reduced form of the product complex: it has the same composition with one extra electron. And thermodynamically it is a good one-electron reductant, due to the stability of the product complex. However it will not be a good reductant kinetically if its oxidation proceeds by way of an unstable semiquinone species. We hypothesize that the reaction complex (reduced R-complex) proceeds, upon removal of one electron at a relatively low potential by cyt. *b*, directly to the oxidized R-complex without passing through any unstable intermediates which would

result in kinetic barriers.

The justification for the hypothesis is that, with a few reasonable assumptions about the properties of the R-complex, it provides a mechanism for enforcing the bifurcated reaction. Let us consider possible pathways to allow both electrons to pass to the high potential chain, violating the bifurcation.

Once the complex has formed, before the electron transfer to cyt. *b*, what could go wrong? Suppose the complex dissociates, where do the electrons go? They cannot both go on the ISP center, as it is a 1-electron carrier. If one electron goes with the ISP leaving the other electron on the semiquinone to react with oxygen or with the ISP on a second cycle, bifurcation would be violated. However this would not happen if the semiquinone is sufficiently unstable: The energy of breaking the bond (separating the spin-coupled electrons, and forming the unstable semiquinone) would make it occur at an insignificant rate. (This is the strong bond between reduced ISP and stable semiquinone proposed by Link [34].) Essentially the quinone is a two-electron carrier, and cannot leave the site in the half-reduced form any more than the ISP can leave in the doubly reduced form. So the only way for the reduced R-complex to dissociate is back to the starting materials, with nothing lost and nothing gained.

Once the first electron has transferred to cyt. *b*, it has to be prevented from escaping back to the high potential chain. There is always the possibility for transferring back to the R-complex as long as it remains, however this just reverses the previous electron transfer and returns to the reduced complex. Once the oxidized R-complex dissociates into reduced ISP and quinone, however, there is no possibility for the electron to return. Even with a favorable ΔG the 10 Å distance reduces the rate to about what is required for

the forward reaction. With a highly unfavorable ΔG due to formation of the unstable semiquinone, the rate would be negligible. So once the R-complex has dissociated, the only way for the electron from heme b_L to come back to the Q_O site would be after reformation of the oxidized R-complex from reduced ISP and oxidized quinone, as happens in EPR titration experiments and as presumably happens during reversed electron transfer experiments. However this is just reversal of the normal reaction, and nothing is lost.

This model avoids one potential problem of all sequential transfer mechanisms with the first electron going to the ISP. This is a possible bypass of the antimycin block by a scheme involving cycles of the normal Q-cycle reaction, in which one electron is transferred to the ISP and the second to cyt. *b*, alternating with perverted cycles in which one electron transfers to the ISP and the resulting semiquinone is reduced by an electron from cyt. *b*.

It must be acknowledged at this point that no new mechanism has been proposed- this is a superset of the schemes of Link [34] and Snyder et al. [38]. However we feel this way of looking at the problem leads to a useful sharpening of the distinctions between two classes of mechanisms: Those in which cyt. *b* is reduced by quinol complexed with the ISP as described here, and those in which quinol reduces the ISP and dissociates giving a short-lived semiquinone that serves as the reductant for cyt. *b*. Consideration of the former mechanisms should focus our attention on the electronic structure of the reduced R-complex and the transition state(s) on the path to the oxidized R-complex. It is expected that proximity of the π-orbital systems in the product complex will allow facile transfer of one electron from quinol to the cluster before or concertedly with transfer of

the other electron to cyt. *b*, avoiding any unstable semiquinone-like species.

Acknowledgments. This work was supported by grant DK44842 from the National Institutes of Health and by the US Dept. of Energy contract DE-AC03-76SF00098 to LBNL. Structural studies of the *Rb. capsulatus* complex leading to the structure in Figure 1 are being carried out in collaboration with Fevzi Daldal of the University of Pennsylvania. The sketch of the Fe_2S_2 cluster and its ligands used in Figure 4 was modified from that on the PROMISE web site (http://metallo.scripps.edu/PROMISE/).

References.

[1] Weiss, H. and Leonard, K. (1987) Chemica Scripta 27B, 73-81.

[2] Xia, D., Yu, C.-A., Deisenhofer, J., Xia, J.-Z. and Yu, L. (1996) Biophysical J. 70, A253.

[3] Xia, D., Yu, C.A., Kim, H., Xia, J.Z., Kachurin, A.M., Zhang, L., Yu, L. and Deisenhofer, J. (1997) Science 277, 60-6.

[4] Zhang, Z. et al. (1998) Nature 392, 677-84.

[5] Kim, H., Xia, D., Yu, C.A., Xia, J.Z., Kachurin, A.M., Zhang, L., Yu, L. and Deisenhofer, J. (1998) Proc Natl Acad Sci U S A 95, 8026-33.

[6] Iwata, S. et al. (1998) Science 281, 64-71.

[7] Hunte, C., Koepke, J., Lange, C., Rossmanith, T. and Michel, H. (2000) Structure Fold Des 8, 669-84.

[8] Hunte, C., Solmaz, S. and Lange, C. (2002) Biochim Biophys Acta 1555, 21-8.

[9] Gao, X. et al. (2002) Biochemistry 41, 11692-702.

[10] Gao, X., Wen, X., Esser, L., Quinn, B., Yu, L., Yu, C.A. and Xia, D. (2003) Biochemistry 42, 9067-80.

[11] Mitchell, P. (1974) FEBS Lett 43, 189-94.

[12] Mitchell, P. (1976) J Theor Biol 62, 327-67.

[13] Palsdottir, H., Lojero, C.G., Trumpower, B.L. and Hunte, C. (2003) J Biol Chem 278, 31303-31311.

[14] Lancaster, C.R. and Michel, H. (1997) Structure 5, 1339-59.

[15] Gurbiel, R.J., Batie, C.J., Sivaraja, M., True, A.E., Fee, J.A., Hoffman, B.M. and Ballou, D.P. (1989) Biochemistry 28, 4861-71.

[16] Britt, R.D., Sauer, K., Klein, M.P., Knaff, D.B., Kriauciunas, A., Yu, C.A., Yu, L. and Malkin, R. (1991) Biochemistry 30, 1892-901.

[17] Rich, P.R. (1989) in: Highlights of Modern Biochemistry, Vol. 1, pp. 903-912 (Kotyk, A., et al., Ed.) V.S.P. Publishers, Prague.

[18] Robertson, D.E., Daldal, F. and Dutton, P.L. (1990) Biochemistry 29, 11249-60.

[19] Trumpower, B.L. (1981) Biochim Biophys Acta 639, 129-55.

[20] von Jagow, G. and Ohnishi, T. (1985) FEBS Lett 185, 311-5.

[21] Ding, H., Robertson, D.E., Daldal, F. and Dutton, P.L. (1992) Biochemistry 31, 3144-58.

[22] Link, T.A., Saynovits, M., Assmann, C., Iwata, S., Ohnishi, T. and von Jagow, G. (1996) Eur J Biochem 237, 71-5.

[23] Darrouzet, E., Valkova-Valchanova, M., Moser, C.C., Dutton, P.L. and Daldal, F. (2000) Proc Natl Acad Sci U S A 97, 4567-72.

[24] Crofts, A.R., Hong, S., Zhang, Z. and Berry, E.A. (1999) Biochemistry 38, 15827-39.

[25] Brugna, M., Rodgers, S., Schricker, A., Montoya, G., Kazmeier, M., Nitschke, W. and Sinning, I. (2000) Proc Natl Acad Sci U S A 97, 2069-2074.

[26] Bowyer, J.R., Edwards, C.A., Ohnishi, T. and Trumpower, B.L. (1982) J Biol Chem 257, 8321-30.

[27] Chain, R.K. and Malkin, R. (1979) Arch Biochem Biophys 197, 52-6.

[28] Crofts, A.R., Shinkarev, V.P., Dikanov, S.A., Samoilova, R.I. and Kolling, D. (2002) Biochim Biophys Acta 1555, 48-53.

[29] von Jagow, G. and Link, T.A. (1986) Methods Enzymol 126, 253-71.

[30] Berry, E.A., Guergova-Kuras, M., Huang, L.S. and Crofts, A.R. (2000) Annu Rev Biochem 69, 1005-75.

[31] Moser, C.C., Page, C.C., Farid, R. and Dutton, P.L. (1995) J Bioenerg Biomembr 27, 263-74.

[32] Crofts, A. and Wang, Z. (1989) *Photosynth. Res* 22, 69-87.

[33] Rich, P.R. (1987) in: Cytochrome Systems: Molecular Biology and Bioenergetics, pp. 495-502 (Papa, S., Chance, B. and Ernster, L., Eds.) Plenum Press, New York.

[34] Link, T.A. (1997) FEBS Lett 412, 257-64.

[35] Gerlt, J.A., Kreevoy, M.M., Cleland, W. and Frey, P.A. (1997) Chem Biol 4, 259-67.

[36] Cleland, W.W. and Kreevoy, M.M. (1994) Science 264, 1887-90.

[37] Meinhardt, S.W. and Crofts, A.R. (1983) *Biochim. Biophys. Acta* 723, 219-30.

[38] Snyder, C.H., Gutierrez-Cirlos, E.B. and Trumpower, B.L. (2000) J Biol Chem 275, 13535-41.

Figure legends.

1. Overall structure of the cytochrome *bc*$_1$ complex. On the left is the vertebrate complex, a homodimer of hetero-11-mers. On the right is the complex of *Rhodobacter capsulatus*, a dimer of heterotrimers containing only the three redox-center-carrying subunits cyt. *b*, cyt. c_1, and the Rieske iron-sulfur protein. The vertebrate complex is a composite of PDB entries 1QRC, 1BBC, and 1BE3. The complex of *Rb. capsulatus* is from a structure currently being refined in the author's lab.

2. Binding of stigmatellin, and proposed binding mode of ubiquinone, in the Q_O site. Panel A shows the binding of stigmatellin in structure 1PPJ. The electron density map is an omit map for stigmatellin, i.e. a Fourier difference map phased using the structure with stigmatellin omitted, to show the shape of the electron density due to the inhibitor. Panel B shows the result of fitting a model for ubiquinone into that density and carrying out positional refinement against the data of 1PPJ, to obtain a model for the binding of ubiquinone in the Q_O site. Protein residues in cyt. *b* are labeled with the 1-letter amino acid code followed by residue number, those in the ISP are preceded by "R:".

3. Cartoon depicting two paradigms for motion of the ISP ectodomain within the catalytic cycle. The ISP is colored by temperature factor, green in the transmembrane helix and better-ordered parts of the ectodomain, fading into yellow and red in the more distal parts of the ectodomain. The Fe_2S_2 cluster is represented by space-filling spheres. Cytochrome *b* is magenta, with blue stigmatellin indicating the Q_O site. The heme of cyt. c_1 is the red ball-and-stick model behind the cluster. The left-hand cartoon depicts the ectodomain as a loosely tethered balloon, buffeted by Brownian motion as it diffuses between binding sites of different affinity. The right-hand model depicts the ISP as part

of an orchestrated machine, with its ectodomain motions conformationally linked to events elsewhere in the complex.

4. Reactant and product complexes at the Q_O site. The reactant complex is formed from reduced ubiquinol and oxidized ISP, however the distribution of the electrons over the two centers in the ground state is unknown. The product complex is formally made by removing one electron from the quinol and transferring the other to the ISP cluster. It is suggested that H-bond between the two reactants constitutes an insignificant barrier to electron transfer, so that the electron is effectively delocalized between the two centers and no unstable semiquinone-like species occurs during oxidation of the reactant complex by cyt. *b*.

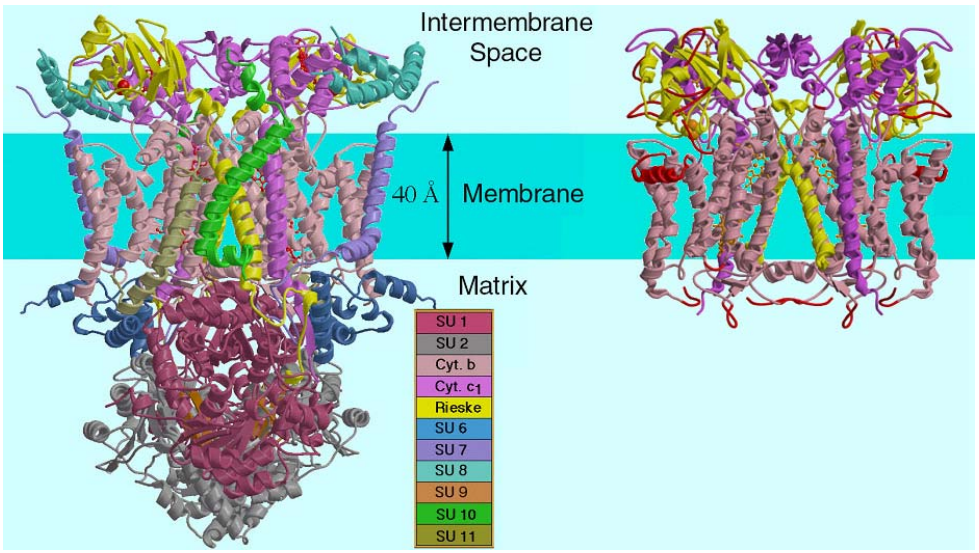

Figure 1.

Figure 1. Overall structure of the cytochrome bc_1 complex. On the left is the vertebrate complex, a homodimer of hetero-11-mers. On the right is the complex of *Rhodobacter capsulatus*, a dimer of heterotrimers containing only the three redox-center-carrying subunits cytochrome b, cytochrome c_1, and the Rieske iron-sulfur protein. The vertebrate complex is a composite of PDB entries 1QRC, 1BBC, and 1BE3. The complex of *Rb. capsulatus* is from a structure currently being refined in the author's lab.

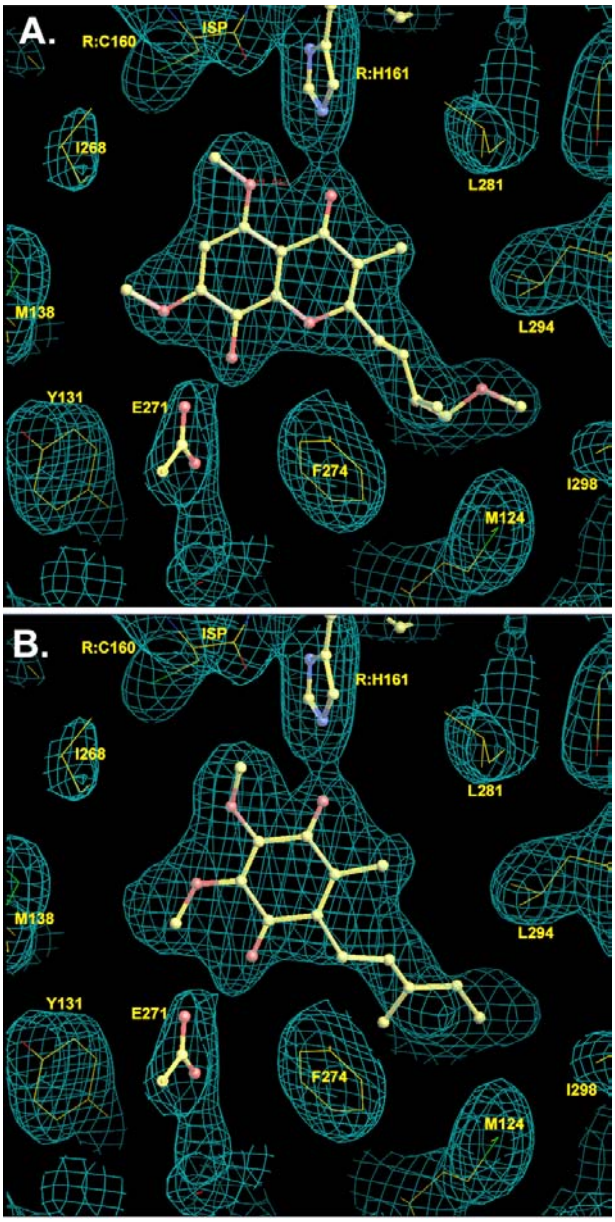

Figure 2

Figure 2. Binding of stigmatellin, and proposed binding mode of ubiquinone, in the Q_O site. Panel A shows the binding of stigmatellin in structure 1PPJ. The electron density map is an omit map for stigmatellin, i.e. a Fourier difference map phased using the structure with stigmatellin omitted, to show the shape of the electron density due to the inhibitor. Panel B shows the result of fitting a model for ubiquinone into that density and carrying out positional refinement against the data of 1PPJ, to obtain a model for the binding of ubiquinone in the Q_O site.

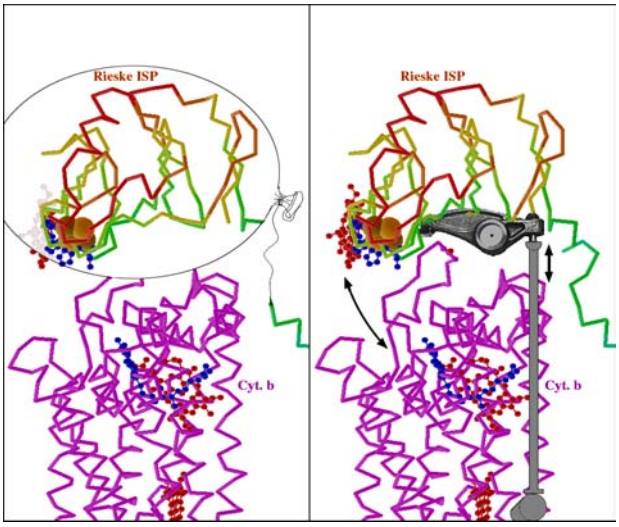

Figure 3

Figure 3. Cartoon depicting two paradigms for motion of the ISP ectodomain within the catalytic cycle. The ISP is colored by temperature factor, green in the transmembrane helix and better-ordered parts of the ectodomain, fading into yellow and red in the more distal parts of the ectodomain. The Fe_2S_2 cluster is represented by space-filling spheres. Cytochrome b is magenta, with blue stigmatellin indicating the Q_O site. The heme of cytochrome c1 is the red ball-and-stick model behind the cluster. The left-hand cartoon depicts the ectodomain as a loosely tethered balloon, buffeted by Brownian motion as it diffuses between binding sites of different affinity. The right-hand model depicts the ISP as part of an orchestrated machine, with its ectodomain motions conformationally linked to events elsewhere in the complex.

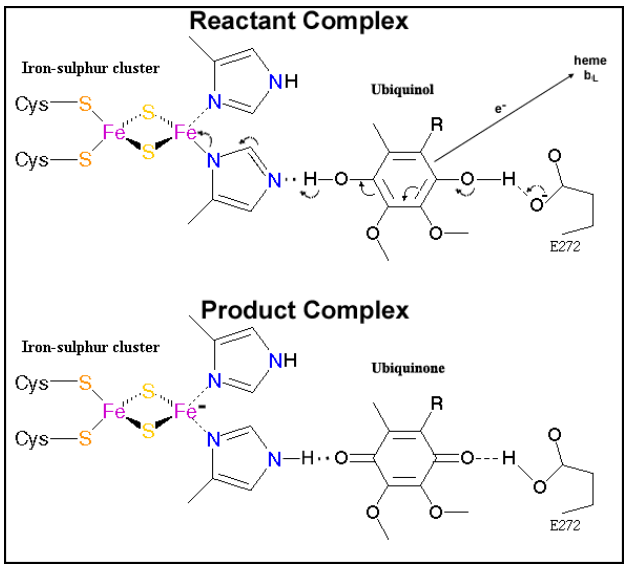

Figure 4

Figure 4. Reactant and product complexes at the Q_O site. The reactant complex is formed from reduced ubiquinol and oxidized ISP, however the distribution of the electrons over the two centers in the ground state is unknown. The product complex is formally made by removing one electron from the quinol and transferring the other to the ISP cluster. It is suggested that H-bond between the two reactants constitutes an insignificant barrier to electron transfer, so that the electron is effectively delocalized between the two centers and no unstable semiquinone-like species occurs during oxidation of the reactant complex by cytochrome b.